

How to perform Flight Vibration Testing based on Operational Modal Analysis?

Jan Schwochow

DLR, Institute of Aeroelasticity, Göttingen, Germany, jan.schwochow@dlr.de

Abstract: Flutter is a dynamic instability caused by the interaction of the structural dynamics of the aircraft and unsteady aerodynamic forces. It occurs when one of the elastic modes of the airframe tends to negative damping above a critical speed. Prediction and flutter clearance are important problems in the design, testing and type-certification of sailplanes. From a practical point of view, Flight Vibration Testing (FVT) needs to be performed whenever a new sailplane is built or an existing type is modified.

The application of Operational Modal Analysis (OMA) methods may provide improvements to identify modal parameters of multiple modes in one step without knowing the type of external excitation. If the identification is repeated for increasing flight velocities, it is possible to find the aeroelastic damping trends and to extrapolate to the stability boundary. The application of OMA needs a broadband excitation spectrum, which result from impulsive control kicks or continuing random excitation like gusts and turbulence in the atmosphere. To demonstrate the performance of the proposed method measured time histories are post-processed to identify all relevant mode shapes with natural frequencies and damping rates of the flying sailplane. Requirements for test equipment, software and the procedure to perform the FVT are summarized.

Keywords: Aeroelasticity, flight vibration test, operational modal analysis.

Introduction

Flutter is a dynamic instability caused by the interaction of the structural dynamics of the glider airframe with control system and unsteady aerodynamic forces induced by the oscillation of the airframe. Depending on the phase lag the resulting forces can amplify the vibration levels above a critical flutter speed. Most flutter problems involve two or more of the following types of vibration modes: bending and torsion of fixed surfaces, rotation and/or torsion of control surfaces and rotation of tabs. Flutter occurs when the aerodynamic damping due to motions in one vibration mode such as wing bending is balanced by the lift due to the angle of attack in another vibration mode such as wing torsion. The primary causes of flutter are as follows:

- Insufficient torsional stiffnesses with center of gravity locations of spanwise sections substantially behind the quarter chords on wings, stabilizers and fins.
- Control surfaces with center of gravity locations of spanwise sections behind the hinge lines and inadequate rigidities in the control systems.
- T-tails which produce unstable coupling between fin torsion and stabilizer yaw with fin bending and stabilizer roll.
- Rotational flexibilities at the roots of all movable horizontal tails which substantially lower the torsional frequencies.

Flutter prediction and flutter clearance are important problems in the design, testing and certification of glider aircrafts. From a practical point of view, the aeroelastic stability must be checked in the flight vibration test (FVT). It needs to be performed whenever a new aircraft is built or an existing aircraft is modified. The procedure of demonstrating that the aircraft is free from flutter in the specified range of velocities and altitudes is called flight envelope clearance. Here, the test pilot tries to excite the glider with impulsive manual control stick jerks and rudder kicks. It is common praxis, that a sufficient decaying response oscillation is evaluated by the judgement of the experienced pilot based on his impression during flight. More reliable methods based on instrumented flutter testing are desirable to reduce remaining risks during test flights.

As a prerequisite for the FVT, it is required to measure the modal parameters of the glider airframe comprising natural frequencies, damping ratios and mode shapes without the impact of aerodynamic forces in the so-called ground vibration test (GVT). The modal parameters are used to obtain the vibration mode shapes, the natural frequencies and structural damping of the airframe for use in the prediction of flutter problems in the rational flutter analysis. It is desirable to have in-flight measurements to compare and calibrate the analysis results, particular for the damping estimates. More sophisticated methods for FVT consist of estimating frequencies and damping ratios of the dynamic pressure dependent aeroelastic modes against the flight speed. The flutter speed is mainly determined by extrapolation of the damping at subcritical speeds. Since damping characteristics often change abruptly near the flutter bound-

ary, it is necessary to evaluate them up to speeds which are very close to the stability boundary. An overview of the methods used in the FVT can be found in [1].

Output-only or operational modal analysis (OMA) techniques have become available in the last years [2] to extract the modal parameters from the dynamic response to operational (ambient) forces, e.g. in flight. Consequently, they deliver a linear (modal) model of the structure around the real working point of operation. The unmeasured, ambient forces are usually modelled as stochastic quantities with unknown parameters but with known behavior, e.g., as white noise time series with zero mean and unknown covariance. The application of OMA may provide improvements to identify modal parameters of multiple modes in one step from measured acceleration response in flight. If the measurement is repeated for increasing flight velocities, it is possible to find the flutter damping trends and to extrapolate to the stability boundary. In OMA all modal parameters are to be determined without knowing the excitation forces. Therefore it is normally assumed that spectral densities of these forces are all flat. It is not essential to satisfy that assumption for the actual physical forces because these acting on the structure can be thought as created by a linear filter loaded by white noise. In this case white noise system input is added with the properties of a linear filter to the system that is going to be identified. Thus the actual physical forces do not need to be white noise or have a flat spectrum, which means that the ambient turbulence in the atmosphere, represented by e.g. the von Karman spectrum [3], might be sufficient to excite glider in the gusty air with thermals (see Figure 1). For demonstration of the performance capabilities, the presented OMA procedure is applied to the recorded in-flight vibration signals of an instrumented FVT.

Figure 2 shows the club-class glider airframe response measured with tri-axial accelerometers during flight at a speed of $V=150\text{km/h}$ in 1300m altitude, which was tried to be constant for 120 seconds. Five span-wise wing stations and the vertical tail were instrumented with MEMS sensors. It provides analog electrical output signals, which are low-pass filtered with cut-off frequency of 50Hz to avoid aliasing effects. The 8x3 signals were recorded and digitized with compact DAQ hardware, which allows simultaneous acquisition of all channels at high sample rates. The aircraft was excited by random impulsive pilot control jerks and rudder kicks and the thermal turbulence, as well.

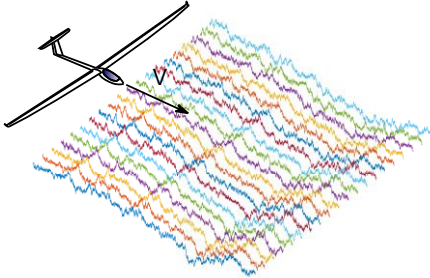


Figure 1. Glider flying in gusty atmosphere

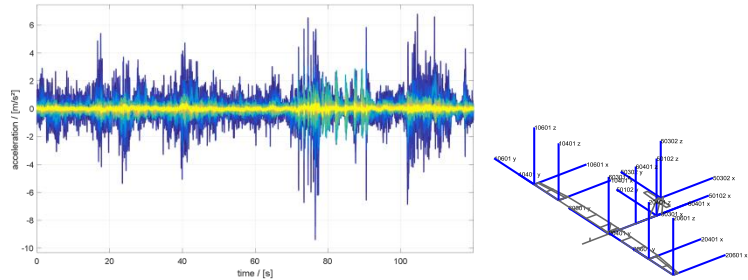


Figure 2. Acceleration response measured in flight at constant flight speed

Methodology

The general modelling procedure numerically linearizes the full nonlinear aeroelastic model represented by the flying glider about the operating point, which comprises current flight speed, flight altitude and trimmed condition including static deformation due to the lifting forces. The linearization routines can be used to develop both a first- and a second-order linearized representation. The complete nonlinear aeroelastic equations of motion can be written as follows:

$$\left[M(\{q\}, \{u\}, t) \right] \{\ddot{q}\} + \{f(\{q\}, \{\dot{q}\}, \{u\}, t)\} = 0 \quad (1)$$

where $[M]$ is the mass matrix, $\{f\}$ is the nonlinear forcing function vector, $\{q\}$ is the vector of displacements, $\{u\}$ is the vector of control inputs, and t is time. Numerically, linearization perturbs all system variables about their respective operating point values. The displacement, velocity, and acceleration perturbation vectors are replaced with the first-order state vector and state derivative vector, in order to determine the first-order representation of the linear time-invariant (LTI)-system:

$$\begin{cases} \{x\} \\ \{\dot{x}\} \end{cases} = \begin{cases} \Delta q \\ \Delta \dot{q} \end{cases}, \quad \begin{cases} \dot{x} \\ y \end{cases} = \begin{cases} \Delta \dot{q} \\ \Delta \ddot{q} \end{cases} \Rightarrow \begin{cases} \dot{x} \\ y \end{cases} = \begin{cases} [A_c] \{x\} + [B_c] \{\Delta u\} \\ [C] \{x\} + [D] \{\Delta u\} \end{cases} \quad (2)$$

In [4] the full derivation of the aeroelastic state-space modelling is presented, where the vibration-induced aerodynamic forces scaled by the dynamic pressure are introduced. If the measurement sampling step Δt is fixed, the continuous state-space model in Eq. (2) can be discretized in time, where k is the index for the time steps. While the inputs $\{u\}_k$ are unknown, the outputs $\{y\}_k$ can be measured e.g. with accelerometers installed at adequate positions on the airframe. The LTI-system of Eq. (2) can now be converted from continuous-time to discrete-time domain by introducing the matrix exponential:

$$\begin{aligned} \{x\}_{k+1} &= [A]\{x\}_k + \{w\}, \quad \text{with } [A] = e^{[A_c](\Delta t)} \\ \{y\}_k &= [C]\{x\}_k + \{v\} \end{aligned} \quad (3)$$

The unknown input terms $\{v\}$ and $\{w\}$ are assumed to be of stochastic type with discrete white noise nature and an expected value equal to zero. For application of the data-driven SSI, first the recorded output data samples plotted in Figure 2 are gathered in a so-called Hankel-matrix:

$$[Y] = \begin{bmatrix} [Y_p] \\ [Y_f] \end{bmatrix} = \begin{bmatrix} \{y\}_1 & \{y\}_2 & \{y\}_3 & \cdots & \{y\}_{N-2q} \\ \vdots & \vdots & \vdots & \ddots & \vdots \\ \{y\}_{2q} & \{y\}_{2q+1} & \{y\}_{2q+2} & \cdots & \{y\}_N \end{bmatrix} \quad (4)$$

Each $\{y\}_k$ contains all accelerations at one certain point in time. The first subset with subscript p expresses the past information and f expresses the future. The subscript q expresses the number of time increments to be used in the analysis, which needs to be pre-selected by the user. N represents the total number of acquired samples. Now, the linear projection from past to future must be represented by the discrete LTI-system in Eq. (3) to be identified. The first step is the orthogonal-triangular decomposition (QR-decomposition) of the Hankel-matrix. Then, the so-called system observability matrix is approximated by singular value decomposition (SVD) of the covariance submatrix between past and future. The dominating part determines the rank of the subspace representing the relevant dynamic system response, while the insignificant part contains the measurement noise. The observability matrix is truncated at the user-selected model order:

$$\begin{bmatrix} [Y_p] \\ [Y_f] \end{bmatrix} = \begin{bmatrix} [L_{11}] & 0 \\ [L_{21}] & [L_{22}] \end{bmatrix} \begin{bmatrix} [Q_1] \\ [Q_2] \end{bmatrix} \Rightarrow [L_{21}] = \begin{bmatrix} [U_1] & [U_2] \end{bmatrix} \begin{bmatrix} [S_1] \\ [S_2] \end{bmatrix} \begin{bmatrix} [V_1]^T \\ [V_2]^T \end{bmatrix} \Rightarrow [O] = [U_1][S_1]^{1/2}. \quad (5)$$

The system matrix $[A]$ is now calculated via least-squares solution, while the output matrix $[C]$ is the first block row of the observability matrix:

$$[A] = [O_1]^* [O_2], [O_1] = \begin{bmatrix} [C] \\ [C][A] \\ \vdots \\ [C][A]^{p-1} \end{bmatrix}, [O_2] = \begin{bmatrix} [C][A] \\ [C][A]^2 \\ \vdots \\ [C][A]^p \end{bmatrix}. \quad (6)$$

The modal parameters of the system are found by performing eigenvalue decomposition of the identified system matrix $[A]$ from Eq. (6). This leads to the discrete-time system poles μ_i with corresponding eigenvectors $\{\psi\}_i$. The damped natural frequencies and damping ratios are calculated from the re-transferred continuous-time system poles:

$$f_i = \frac{\text{Im}(\lambda_i)}{2\pi}, \quad \zeta_i = -\frac{\text{Re}(\lambda_i)}{|\lambda_i|}, \quad \text{with } \lambda_i = \frac{\ln(\mu_i)}{\Delta t}, \quad \{\phi\}_i = [C]\{\psi\}_i \quad (7)$$

All applied mathematical functions - QR-decomposition, SVD-decomposition and eigenvalue-decomposition - are standard matrix algebra routines, which are available from most mathematical software libraries. An introduction in signal processing and vibration analysis is given in [5], which is accompanied by a software toolbox for the free mathematical software GNU/Octave [6].

Results

The acceleration response data from flight test plotted in Figure 3 are analyzed with the presented OMA method above. The number of time increments in Eq. (4) is chosen to 12, while the model order in Eq. (5) – the number of singular values representing the orthogonal subspace of the Hankel matrix – is set to 120. Table 1 contains the 17 identified natural frequencies and dampings calculated via Eq. (7). Two of the identified mode shapes are plotted in Figure 3. Mode 2 is the fundamental bending of the glider wing at frequency 2.45Hz. The aeroelastic damping is high with 20.5%, which results from the motion-induced aerodynamic forces acting as damping force for heave motion. Usually the structural damping values of a glider airframe measured in the GVT are all below 2%. The second mode is symmetrical fuselage bending at 10.74Hz. As can be seen from Table 1 the presented algorithm is able to identify mode shapes with natural frequencies up to 30Hz with comparable high damping rates. Generally, this range covers the symmetric and antisymmetric wing torsion modes of glider airframes, which are most important to be monitored in the flutter analysis.

| No. | Name | freq. Hz | damp. % |
|-----|---------------------------------------|-------------|------------|
| 1 | rigid-body heave | 0.75 | 62.88 |
| 2 | sym. 1 st wing bending | 2.45 | 20.50 |
| 3 | anti. fuselage against wing | 4.00 | 8.54 |
| 4 | sym. in-plane wing bending | 4.69 | 13.21 |
| 5 | anti. 1 st wing bending | 6.24 | 6.47 |
| 6 | anti. htp roll | 7.30 | 9.04 |
| 7 | sym. 2 nd wing bending | 8.89 | 9.13 |
| 8 | sym. fuselage bending | 10.74 | 5.17 |
| 9 | sym. in-plane bending | 11.78 | 2.83 |
| 10 | anti. horizontal tail bending | 12.56 | 5.53 |
| 11 | anti. 2 nd wing bending | 15.73 | 4.26 |
| 12 | anti. in-plane bending | 17.58 | 5.57 |
| 13 | sym. 3 rd wing bending | 18.71 | 4.25 |
| 14 | sym. 2 nd fuselage bending | 21.84 | 4.54 |
| 15 | anti. in-plane bending | 22.96 | 2.88 |
| 16 | sym. in-plane bending | 26.45 | 3.18 |
| 17 | anti. wing torsion | 28.93 | 4.27 |

Table1. OMA-identified frequencies and dampings

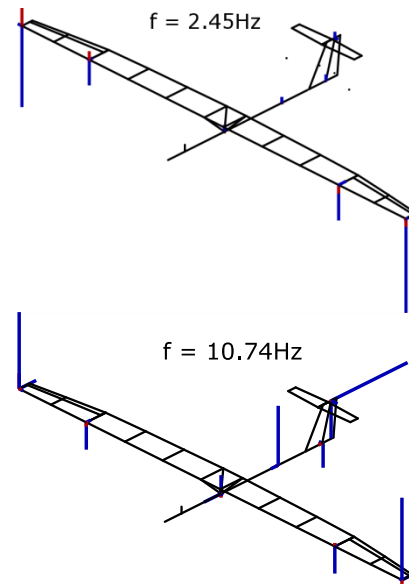


Figure 3. OMA-identified mode shapes

Conclusion

The application of OMA methods to evaluate flight vibration acceleration response data is presented, which needs unknown random excitation of the glider in flight by random pilot control inputs and atmospheric turbulence. The advantage of OMA may provide improvements to identify modal parameters of multiple modes in one step which is infeasible by manual pilot monitoring during flight testing. If the identification process is repeated for increasing flight velocities, the aeroelastic damping trends can be evaluated, extrapolated towards the flutter stability boundary and compared to the rational analysis.

References

- [1] Meijer, J.J. Introduction to Flight Test Engineering - Aeroelasticity. RTO AGARDograph 300 Vol.14 (2005).
- [2] Brincker, R. Some Elements of Operational Modal Analysis, Shock and Vibration, vol. 2014, Article ID 325839, 11 pages, (2014). doi:10.1155/2014/325839
- [3] Hoblit, F. M. Gust Loads on Aircraft: Concepts and Applications. Washington, DC: American institute of Aeronautics and Astronautics, Inc. (1988). ISBN 0930403452.
- [4] Schwochow, J., Jelcic, G. Automatic Operational Modal Analysis for Aeroelastic Applications. 6th International Operational Modal Analysis Conference IOMAC, 12-14 May, Gijón, Spain (2015).
- [5] Brandt, A. Noise and Vibration Analysis: Signal Analysis and Experimental Procedures, Wiley and Sons., (2011).
- [6] <https://www.gnu.org/software/octave/>.